Scanning Microscopy Vol. 12, No. 1, 1998 (Pages 81-91) 0891-7035/98$5.00+.25
Scanning Microscopy International, Chicago (AMF O'Hare), IL 60666 USA

SIMULATIONS OF HOMOEPITAXIAL GROWTH OF PT(111): ISLAND SHAPES AND THE GROWTH MODE

J. Jacobsen[1]*, K.W. Jacobsen and J.K. Nørskov

Center for Atomic Scale Materials Physics and Department of Physics,
Technical University of Denmark, DK 2800 Lyngby, Denmark

(Received for publication May 28, 1996 and in revised form September 17, 1996)

Abstract

Experimental observations of homoepitaxial growth of Pt(111) have shown a surprising richness of transitions in the island shape and the growth mode as functions of temperature. We present a set of kinetic Monte Carlo simulations capable of reproducing the various observed dendritic and compact island shapes, and the unexpected transition to reentrant layer by layer growth. The simulations are based on the available experimental information, and Effective Medium Theory energy barrier calculations. The variations in island shape are explained in terms of the mobility and stability of adatoms and rows of atoms attached to the island edges, and the transition to reentrant layer-by-layer growth is found to be caused by a transition in the island shape.

Key Words: Pt(111), homoepitaxial growth, effective medium theory, island density, island shape transitions, growth mode transition, step edge diffusion, corner diffusion, energy barriers.

[1]Current address: Laboratory of Atomic and Solid State Physics, Cornell University, Ithaca, New York.

*Address for correspondence:
Joachim Jacobsen
Haldor Topsoe A/S
Nymollevej 55
DK-2800 Lyngby, Denmark
Telephone Number: +45-45272734
E-mail: jcj@topsoe.dk

Introduction

Homoepitaxial growth of Pt(111) has recieved considerable attention in the crystal growth community. The reason is the observations of striking variations in the island density [4, 5, 27], island shape [12, 24] and the growth mode [5, 18, 26] with the substrate temperature, and the existence of a growth induced reconstruction of the surface [4, 8]. Depending on the temperature and deposition rate, the surface can grow in either a 2-dimensional (2D, layer-by-layer) or 3-dimensional (3D) growth mode [18], and the islands nucleated during the growth may take on a variety of fractal, triangular or hexagonal shapes [24]. In particular, the transition from 3D growth around 400 K to reentrant layer-by-layer or 2D growth at lower temperatures is interesting because of its relevance to the general goal of being able to grow smooth thin films. The experimental observations of the system have triggered a considerable amount of theoretical work including various first-principles [9, 10, 25] and more approximative [14, 15, 19, 21, 31, 32] total energy calculations, molecular dynamics simulations [33, 34] and kinetic Monte Carlo (kMC) simulations [5, 12, 13, 14, 20, 36].

The shape of the islands of monoatomic height formed during homoepitaxial growth of Pt(111) has been measured using Scanning Tunneling Microscopy (STM) [12, 24]. For typical deposition rates of 10^{-3} to 10^{-2} ML/s, there is a transition at around 300 K from a fractal or dendritic island shape to a compact island shape when increasing the temperature. However, an equilibrium island shape is only obtained when the substrate temperature is increased to 710 K. In between, the compact islands take on various different triangular and hexagonal shapes. At 400 K the islands are triangular and surrounded by so-called A-step edges (see Fig. 1). At 455 K the islands are hexagonal and surrounded by both A- and B-step edges. At 640 K the islands are again triangular, but at this temperature they are surrounded by B-step edges, i.e., the triangles are rotated by 180°. The equilibrium island shape is quasi-hexagonal, with the B-step edges longer than the A-step edges, and from this shape one can deduce the ratio of free energies of the two types of step edges to be $\varepsilon^{B}_{step}/\varepsilon^{A}_{step} = 0.87 \pm 0.02$ [23, 24]. In [13] we present a growth model which reproduces the observed compact island shapes in the temperature range from below 400 K to 800 K, and which

suggests an explanation of these compact island shapes in terms of step energies, and binding energies of single atoms and rows of atoms attached to the steps.

For low deposition fluxes (6.7 x 10^{-4} ML/s), the low temperature islands are not random fractals, but rather they are dendrites, and the island branches have preferred growth directions perpendicular to the A-steps [12]. The island shape is modeled by assuming an asymmetry in the diffusion of atoms away from the corners of the islands, similar to what is suggested to happen for the growth of Ag on Pt(lll) [6].

Homoepitaxial growth of Pt(lll) is known to proceed in a 2D fashion around 620 K, a 3D fashion around 425 K, and then again in a 2D fashion around 275 K [5, 18]. The high temperature growth mode transition can be understood by the presence of a Schwoebel barrier [15, 28, 37], which is the additional energy barrier atoms have to overcome in order to descend from islands on the growing surface. If, at some low temperature the atoms can not overcome this barrier, 3D growth will result [30]. The low temperature growth mode transition to the so-called reentrant layer-by-layer growth is harder to rationalize. If transient interlayer mobility of the deposited atoms is sufficiently high at low temperatures, where there is a very high step density, it could be the mechanism behind the growth mode transition [1], however molecular dynamics simulations do not support this hypothesis [33]. The low temperature growth mode transition can then only be explained if the Schwoebel barrier is lowered or not present at the lower temperatures. In reference [15] we present a growth model, based on scaled Effective Medium Theory (EMT) [16, 17, 29] energy barriers for the atomic diffusion which is able to reproduce the transition to reentrant layer-by-layer growth. We found that the transition is strongly coupled to the transition in island shape from compact triangular islands around 400 K to fractal islands at lower temperatures. Along the irregular edges of the fractal islands, special sites with a low Schwoebel barrier can be found.

The growth models mentioned above are all formulated in terms of a set of energy barriers for atomic diffusion events and it is not immediately obvious that they are internally consistent. In this paper, we present a model which is able to reproduce experimental island densities, all the observed dendritic and compact island shapes, and the growth mode transition from 3D growth around 400 K to reentrant layer-by-layer growth at lower temperatures. We formulate a consistent set of mechanisms which we show can give rise to the observed growth behavior. Essentially all available experimental and theoretical information about the system is used in constructing the set of energy barriers in the model. We emphasize the consistency of the model, and the good agreement with experiment, but do not claim to predict the exact values of energy barriers. For the variations with temperature of compact island shapes, our proposed mechanism may not be the only possibility.

The paper is organized as follows: First, we briefly explain the method used in the simulations. Then we establish a useful nomenclature which will ease the following discussion. Having done that, we turn to presenting the growth model and the outcome of simulations of the model at varying surface temperature and deposition rate. As we do this, we discuss the mechanisms, which give rise to the changes of island shape and growth mode in the model. We also mention the possibility of alternative mechanisms. Finally, we conclude with a brief summary.

Method

We simulate the homoepitaxial growth of Pt using kMC [11, 22, 35]. The simulations are done on an fcc lattice. For a given configuration of the surface, a list of all possible atomic diffusion processes and their corresponding rates is created. One of these processes is then chosen to occur with a probability proportional to its rate, or a new atom is deposited with a probability proportional to the total deposition rate. The list of processes is updated, a new event is chosen and so forth. The possible atomic diffusion processes are given by the growth model described below. The rates of these processes are assumed to be given by $r_i = \nu \exp(-E_i/kT)$, where k is the Boltzmann constant, T is the temperature, and E_i is an energy barrier, which depends on the local environment. A common pre-exponential of $\nu = 10^{12}$ s^{-1} is assumed for all processes. Overhangs are neglected and hence atoms funnel down until they are supported by three neighbors below.

For the EMT calculations, details of the implementation and the actual parameter values can be found in reference [29].

Nomenclature

Because we neglect overhangs, the possible diffusion processes naturally divide into *in-layer* and *inter-layer* processes, where the layers are the (111) planes parallel to the surface. *In layer* processes can be diffusion of isolated atoms on the terrace (*terrace diffusion*), diffusion of atoms along island edges (*edge diffusion*) or dissociation of atoms from island edges to the terrace (*2D-evaporation*). Important characteristics of *in-layer* processes are the number of nearest neighbors in the same layer of the moving atom in its initial and final state. We label these numbers N_i and N_f. For terrace diffusion N_i is always zero, for edge diffusion N_i and N_f are greater than zero, and for 2D evaporation N_i is greater than zero, while N_f is zero.

Of particular importance to the island shape are the edge diffusion processes. In Figure 1a, we define various structures found along the island edges. Note first of all the difference between the two types of straight steps on the (111) surface: the *A-step* made up of a (100) facet, and the *B-*

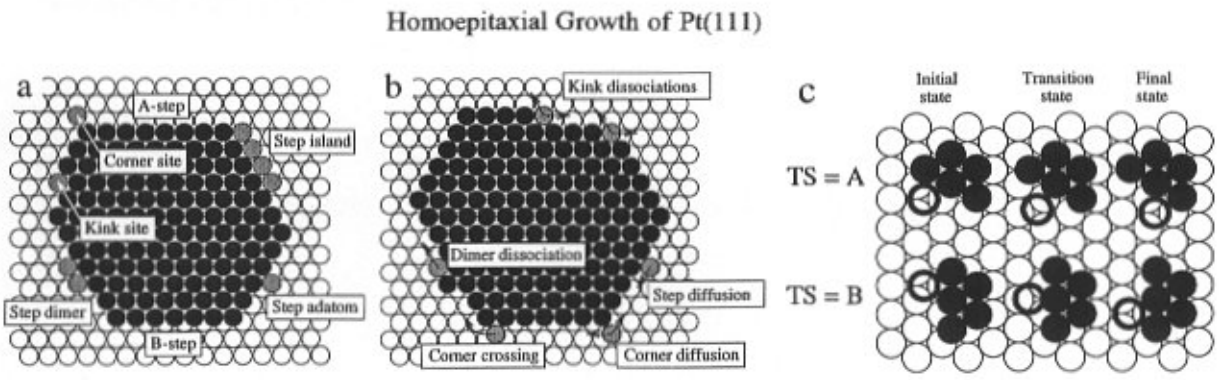

Figure 1. (**a**) Structures of atoms attached to island edges and special sites the adatoms can occupy. (**b**) Various edge diffusion processes important for the island shape. (**c**) The transition state for diffusion along A- and B-steps.

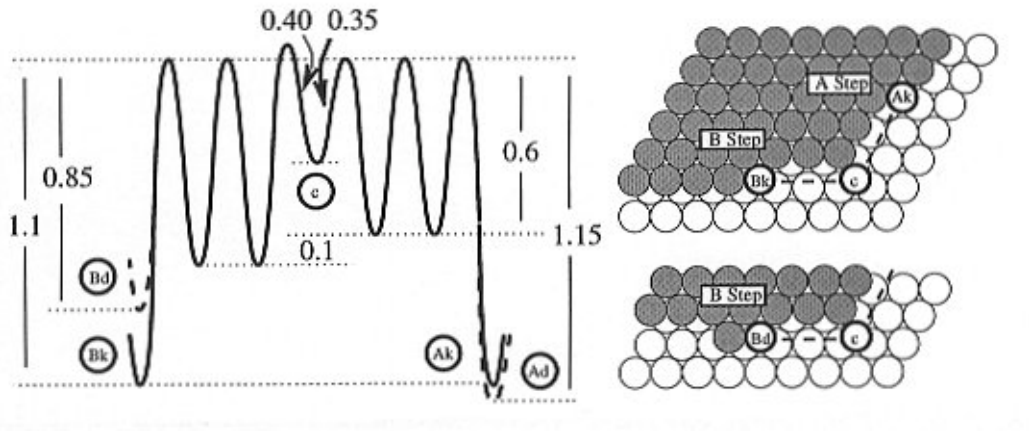

Figure 2. The energy barriers in eV for edge diffusion, as used in the kMC simulations. The solid curve on the left shows the potential energy of an atom which is displaced from a kink site at the B-step (Bk) via a corner site (c) to a kink site at the A-step (Ak). The dashed curves show how the kink dissociation barriers are changed if the atom is initially part of a step dimer (Ad and Bd on the A and B steps, respectively. The atomic configurations are shown on the right.

---

step made up of a (111) facet. A *step island* is a row of atoms attached to an island edge. The smallest step island is the *step dimer*. A single atom attached to an island edge is a *step adatom*. A special site for a step adatom is the *corner site*, in which the adatom only has one neighbor in the island. When the step adatom diffuses to a *kink site*, it becomes part of a step island. In Figure 1a we define various edge diffusion processes. For *corner diffusion*, N_i is 1. For *step diffusion* N_i is 2, the two neighbors must themselves be neighbors to form a part of a step, and the moving atom must diffuse along one of its neighbors. For *kink dissociations* N_i is 3, the three neighbors must form a kink, and the moving atom must diffuse along one of its neighbors. A *dimer dissociation* is a kink dissociation, in which a step dimer breaks up. Since an atom undergoing an edge diffusion process (as defined above) always diffuses along exactly one in-layer neighbor, the transition state (*TS*) is always similar to either A-step diffusion of B-step diffusion. Hence, the edge diffusion process can be labeled with a *TS*, where *TS* is either A or B. This is illustrated in Figure 1c. With these definitions, we can label an edge diffusion process by $N_i TS N_f$. For example, diffusion along a straight A-step is labeled 2A2. We will use E for energy barriers, and ε for energy levels, or differences in energy levels of meta-stable states.

Table 1. Energy barriers in eV used in the model which reproduces island densities, island shapes and the growth modes.

Terrace diffusion				
Diffusion of monomers				0.26
2D Evaporation				
Dissociation from 1 in layer neighbor				0.8
Edge diffusion	N_i	*TS*	N_f	
Corner diffusion	1	A	≥1	0.35
Corner diffusion	1	B	≥1	0.40
Step Diffusion/Step to corner	2	A	> 1	0.60
Step to corner	2	B	1	0.75
Step Diffusion	2	B	> 1	0.70
Kink Dissociation	3	A	≥ 1	1.10
Kink Dissociation	3	B	1	1.15
Kink Dissociation	3	B	> 1	1.10
Step dimer dissociation	3	A	≥ 1	1.15
Step dimer dissociation	3	B	1	0.90
Step dimer dissociation	3	B	>1	0.85
Inter-layer diffusion				
Descent at straight step				0.6
Descent next to kink at B-step				0.34

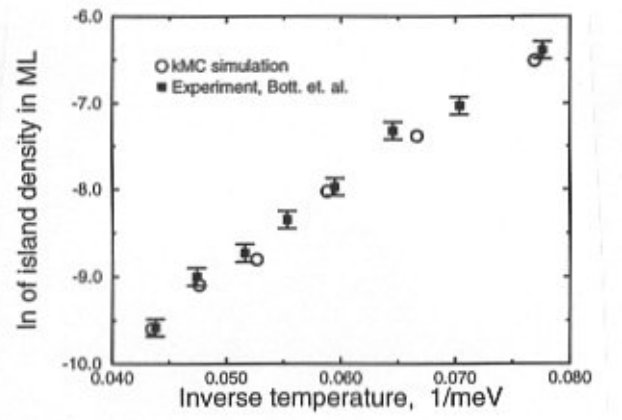

Figure 3. Natural logarithm of the simulated and measured saturation island densities as a function of inverse temperature for temperatures below 270 K. In both cases, the deposition is flux 0.00066 ML/s. The experimental data is from reference [4].

Pt/Pt(111) Growth Model

The atomic diffusion processes included in the model are listed in Table 1 together with their corresponding energy barriers. Only single atom events are included in the model. Dimers are explicitly immobile, thus the corner diffusion is not active in the case of a dimer. Figure 2 shows an energy diagram for edge diffusion constructed from Table 1. A common pre-exponential of 10^{12} s^{-1} is used for all processes. In the case of adatom terrace diffusion, this pre-exponential is the attempt rate for jumping from an fcc site to each of the six neighboring fcc sites.

The model parameters are, as far as possible taken from [13] and [15]. The edge diffusion barriers are taken from [13], with the details at the corners changed to also reproduce the shape of the low temperature dendritic islands. When comparing the barriers for the inter-layer processes with those given in [15], some care should be taken: In the present model, for reasons of simplicity, we do not include the lowering of the energy level of atoms on an island when they approach the descending step edge. This lowering is found in the EMT [15], in Embedded Atom calculations [32] and in Field Ion Microscopy (FIM) experiments for other systems (see reference [7] and references herein), but is not essential for reproducing the transition to reentrant layer-by-layer growth. Therefore, the inter-layer barriers in this model are from an 0.06 eV higher energy level, than those in [15].

The island density

Bott *et al.* [4] report very carefully performed nucleation experiments for Pt/Pt(111) using an STM and can reproduce the measured saturation island densities using 5 x 10^{12} s^{-1} and 0.26 eV for the pre-exponential and energy barrier for the terrace

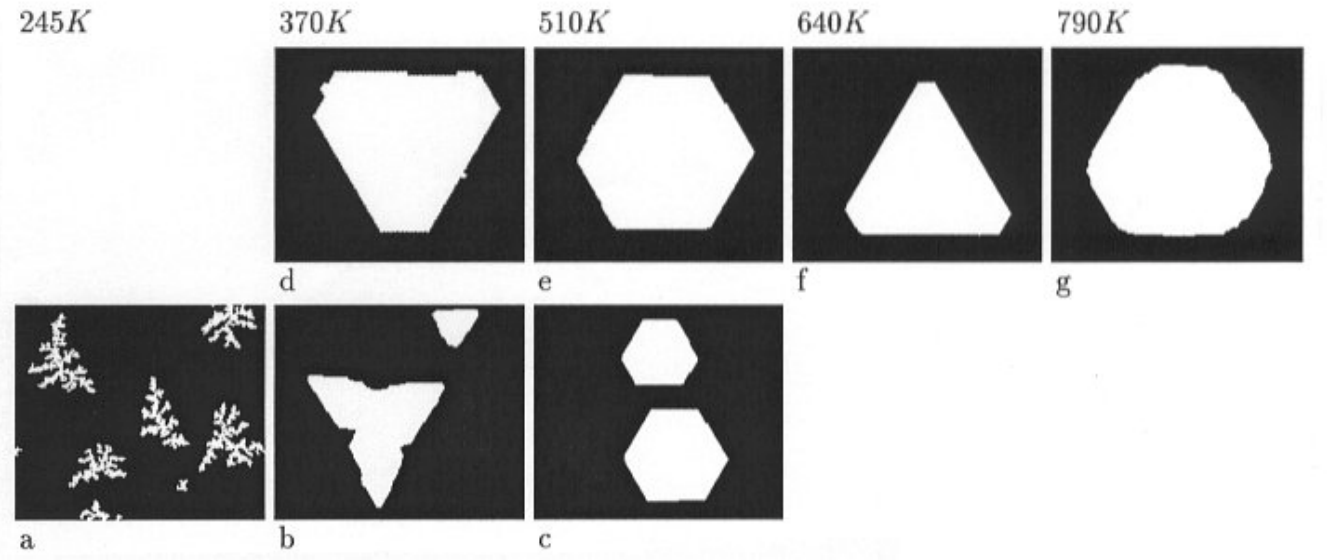

Figure 4. Simulated island shapes as a function of temperature. The surface orientation is as in Figure 1a. Below: Random deposition on the terrace. Only part of the simulated surface is shown. (**b**) and (**c**) are not reprsentative of the island density. Deposition Flux F, coverage O and shown area A: (**a**) F=O.OOO2 ML/sec, O=0.1 ML, A=9OOOO unit cells; (**b**) F=O.OO1 ML/sec, O=0.06 ML, A=324OO unit cells; (**c**) F=0.001 ML/sec, O=0.04 ML, A=28900 unit cells. Above: random deposition directly along the island edge. Deposition flux: O.OOl ML/s. Total deposition rate R, island size S and the coverage O: (**d**) R 22.5 atom/s, S = 1157 atoms, O = 0.05 ML; (**e**) R = 140.6 atom/s, S = 7OOO atoms, O = 0.05 ML; (**f**) R = 360 atom/s, S = 18000 atoms, O = 0.05 ML; (**g**) R = 722.5 atom/s, S = ll241 atoms, O = 0.016.

diffusion of isolated adatoms in kMC simulations. In Figure 3 we compare the saturation island densities obtained within the present model to their experimental data. The temperature range is 150 to 270 K, and the deposition flux is 6.6 x 10^{-4} ML/s, in both experiment and simulation. The agreement is excellent. The model barrier for 2D-evaporation from 1 in-layer neighbor of 0.8 eV makes dimers stable in the entire temperature range (the process does in fact not influence any of the simulations presented here). The agreement in Figure 3 justifies that dimers are stable and immobile up to 270 K.

The island shape

Figure 4 shows the simulated island shapes as a function of surface temperature and deposition flux. These simulations are done in two different ways. At the higher temperatures, it is not possible to simulate the diffusion of isolated atoms on the terrace. The ratio of their hopping rate to the deposition rate is too unfavorable for the kMC simulation. In Figures 4d through 4g, the atoms are deposited directly at a random place along the island edge, and only the edge diffusion processes are in-cluded. The total deposition rate is inversely proportional to the island density, where we have used a simple interpolation of values obtained from Figure 1b and 1d of reference [24]. In Figures 4a through 4c, the atoms are deposited randomly on the entire surface, and all processes of Table I are included.

By comparison to the STM images in references [12] and [24], the model clearly reproduces the experimental island shapes very well. At 245 K and 2 x 10^{-4} ML/s the simulated islands are dendritic with a triangular envelope. The island branches preferentially grow perpendicular to the A steps. Upon raising the temperature, the islands become compact. At 370 K the simulated islands are triangular having A-steps. At 640 K the islands are triangular having B-steps. At 510 K the simulated islands are hexagonal, and at 790 K the islands are quasi-hexagonal, with the B-step edges longer than the A-step edges, and with rounded corners.

At 510 K there is very little difference between the two ways of doing the simulation (Figs. 4c and 4e). Because of the high mobility of step adatoms, it is not important where the atoms first attach to the island. This will be true also for higher temperatures. At 370 K there is a significant difference between the two ways of doing the simulation. The islands in Figures 4b and 4d are both mainly surrounded by A-steps. But the island in Figure 4b has sharper tips, and concave step edges. There are two reasons for this. Because of the character of the random walk of the diffusing adatoms on the terrace,

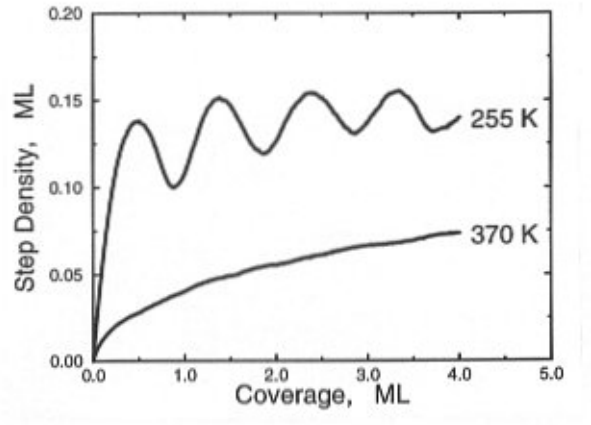

Figure 5: The simulated step density as a function of coverage at 255 K and at 370 K. The oscillations indicate layer-by-layer growth, and the monotone increase indicates multilayer growth. The deposition rate is 0.01 ML/sec.

---

they will be more likely to attach to the tips rather than the sides of the triangular islands. But also, due to the non-uniformity in the inter-layer barrier, (which we will address below), the atoms arriving on top of the islands will predominantly descend at the tips, as long as second layer nucleation has not yet set in. Both of these mechanisms will increase the growth velocity of the tip relative to the sides, and this gives the islands their characteristic shape with the concave sides.

We now discuss the mechanisms which give rise to the various island shapes in the model. To do this, we use the EMT result, that the energy barrier for edge diffusion in general increases with N_i [15]. Consequently, at the lowest temperatures, only processes with low N_i are active and can influence the island shape. As the temperature increases, additional processes become active in order of increasing N_i.

It is possible to imagine a temperature where terrace diffusion is the only active diffusion process, and all edge diffusion is frozen, i.e., where only N_i=0 processes are active. In this case, classical diffusion limited aggregation will be observed [6, 38]. When increasing the temperature, corner diffusion with N_i=1 will be the next process to become active. If the barrier for corner diffusion is the same towards the A- and the B-step, this process will give rise to a slight increase in the arm width of the fractal islands [12, 39]. If these barriers are not the same, step adatoms at corner sites will preferentially diffuse in the direction of the lower barrier. This will give rise to preferred growth directions of the island branches [6, 12], with the island branches growing faster in the direction perpendicular to the step to which the step adatoms tend to go. We use the barriers 0.35 and 0.40 eV for the corner diffusion towards the A- and the B-step respectively. This makes the island branches grow faster perpendicular to the A-step (Figure 4a). It is a relatively weak asymmetry, and it is necessary to go to a very low deposition flux to see a strong effect in agreement with experiment [12, 24]. Hohage *et al.* [12] suggest the barriers 0.33 and 0.51 eV for the same two processes, with a pre-exponential of $5 \times 10^{12} s^{-1}$.

When further increasing the temperature, edge diffusion processes with N_i=2 are the next processes to be activated. This allows for step diffusion and corner crossing, and when these processes are sufficiently fast, a compact island will grow. Step adatoms can move as long as they are isolated, but are immobile after arriving at a kink site. The important quantities become the mobilities, given by E_{2A2} and E_{2B2}, of step adatoms along the two types of steps, and the relative stability on the two steps. The latter is given by $\Delta\varepsilon_1$, the difference in the total barrier for corner crossing when coming from the two different steps. We write $\Delta\varepsilon_1 = \varepsilon^A_1 - \varepsilon^B_1$ where ε^A_1 is the energy level of a step adatom on the A-step compared to the bulk energy level, and likewise for ε^B_1.

The diffusion barriers for Pt adatoms along the rows on the Pt(311) and Pt(331) surfaces have been measured using FIM to be $E_{311} = 0.69 \pm 0.2$ eV and $E_{331} = 0.80 \pm 0.1$ eV [2]. These diffusion processes are very similar to the diffusion along A- and B-steps respectively. This suggests that $E_{2A2} < E_{2B2}$. In [13] it is shown how $E_{2A2} < E_{2B2}$ with $\Delta\varepsilon_1 = O$ will cause the A-step to be the faster growing step and give rise to islands with B-step edges longer than A-step edges. With $E_{2A2} < E_{2B2}$, it is essential to have $\Delta\varepsilon^1 > 0$, in order to reproduce the experimental island shape around 400 K. This is also found by Villarba [31]. This stronger binding of the adatoms to the B-steps will give a net rate of corner crossing from the A- to the B-step. The B-steps will then grow faster, leaving behind a triangular island surrounded by A-steps. Based on the experimental values for E_{311} and E_{331}, and on the scaled EMT barriers from [15], we use $E_{2A2} = 0.6$ eV and $E_{2B2} = 0.7$ eV. Higher values will give a too high transition temperature to compact islands. With $\Delta\varepsilon_1$=0.1 eV we reproduce the experimental island shape around 400 K (Fig. 4b).

When increasing the temperature even further, the kink dissociations with N_i=3 become activated. This enables step islands to redissociate, and the relative binding of step islands on the two steps becomes relevant. While the assumption that step adatoms bind the strongest to the B-step seems to be what causes the growth of triangular islands having A-steps around 400 K, it is in fact an anomaly compared to what would be expected from the experimental ratio of the step energies ($\varepsilon^B_{step}/\varepsilon^A_{step} < 1$). In ref. [13], the relation between the binding energies of step islands and the step energies is explored, and it is concluded, that if one neglects differences in the interaction between kinks on the two different steps, it follows that

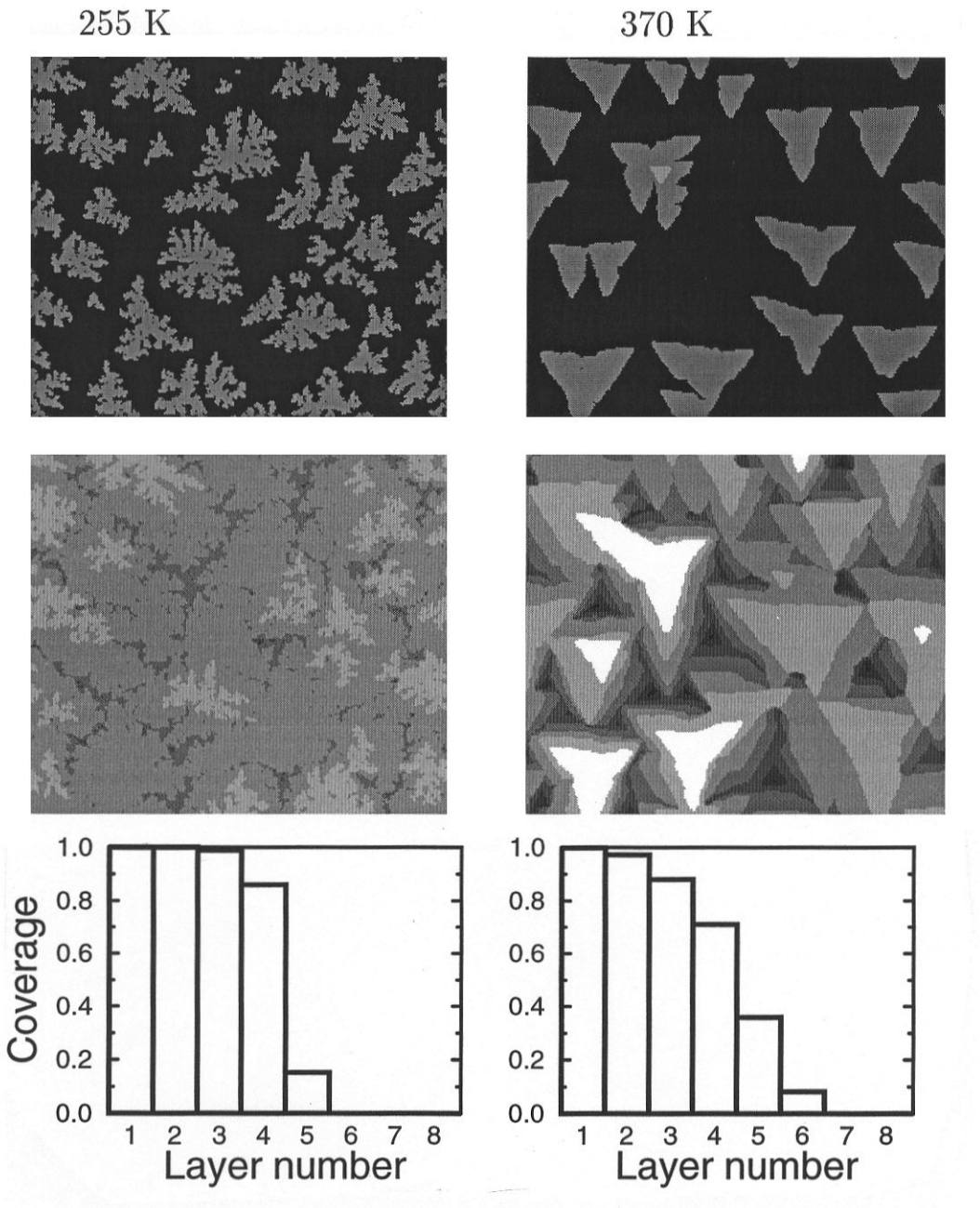

Figure 6: Surface morphologies after simulated deposition of 0.25 ML (top) and 4ML (below) at 255 K (left) and 370 K (right) at a deposition flux of O.O1 ML/sec. The surface orientation is as in Figure 1a. The surface areas are 4OO x 4OO surface unit cell at 255 K and 5OO x 5OO at 37O K. Also shown are histograms of the coverage in each layer above the surface at the total coverage of 4 ML.

$$3(\varepsilon^{A}_{step} - \varepsilon^{B}_{step}) = \varepsilon^{B}_{N} - \varepsilon^{A}_{N}, \qquad (1)$$

where ε^{A}_{N} is the energy level with respect to bulk Pt atoms of an N-sized step island on the A-step, ε^{A}_{step} is the energy of A-steps per step atom, and likewise for ε^{B}_{N} and ε^{B}_{step}. Hence, the N-sized island bind stronger to the less stable step, which is the opposite of our assumption for the step adatom. The assumption for the kink-kink interactions, which leads to eq. (1) need not be valid for small *N*.

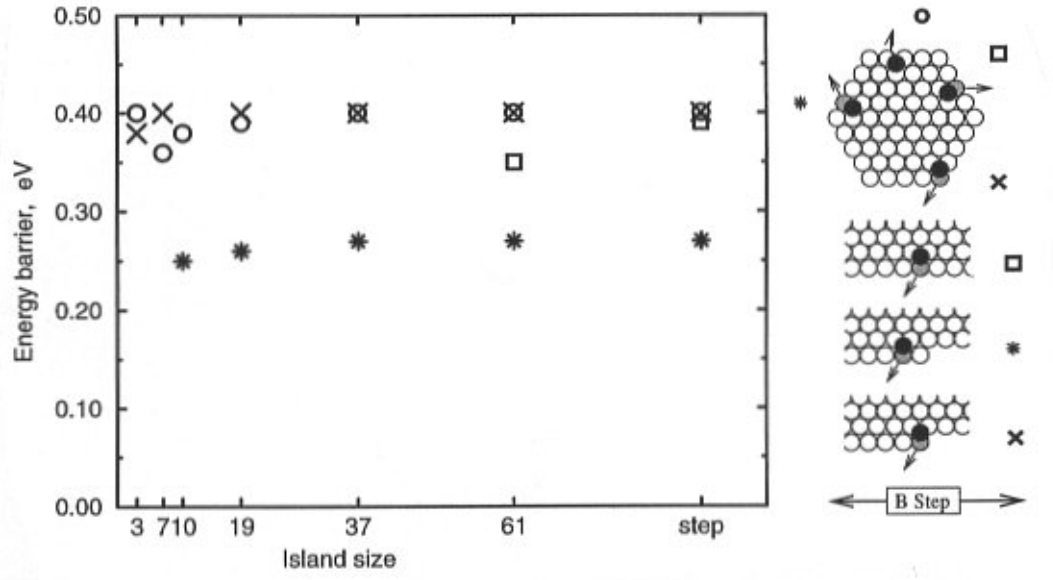

Figure 7: EMT energy barriers for atoms descending from compact islands of various sizes, and from straight steps. The different symbols correspond to the different local environments shown to the left. These are over-edge descents at A-steps (circle) and various exchange descents at B-steps (square, star, cross).

Any kMC model attempting to describe the scenario of islands observed in [24] must be consistent with the step energies governing the island shape in the high temperature limit. Insisting on our assumption for the binding of step adatoms, the simplest possible model is to assume that the step dimers (and longer step islands) behave according to eq. (1). To obtain this result, we must introduce kink interactions in a step dimer which are different on the two steps. Apart from this, and for reasons of simplicity, we have no other kink interactions in the model. Within this model we have the result [13] that

$$\varepsilon^{A}_{step} = 1 \text{ over } 3\ \varepsilon^{A}_{N} + 2 \text{ over } 3\ \varepsilon^{B}_{N} \qquad (2)$$

for $N \geq 2$, and likewise for ε^{B}_{step}. With the edge diffusion barriers given in Table I we have $\varepsilon^{A}_{N} = 0.45$ eV and $\varepsilon^{B}_{N} = 0.65$ eV. Using Eq. 2, we find $= 0.58$ eV/atom, $\varepsilon^{B}_{step} = 0.52$ eV/atom and $\varepsilon^{B}_{step}/\varepsilon^{A}_{step} = 0.89$ consistent with the experimental value. The magnitudes of the step energies are approximately 10% of the bulk energy for Pt (5.85 eV/atom), which is a very reasonable number [9].

With step adatoms more stable on the B-step, and step dimers more stable on the A-steps, the dissociation of step dimers on the B-step is the kink dissociation with the lowest energy barrier, and thus, the first kink dissociation to be activated when increasing the temperature. When this happens the growth of the B-steps slows down compared to the A-step because the nucleation of step islands slows down. The A-step becomes the faster growing step and the growing island becomes triangular and surrounded by B-steps. In the model this happens at 640 K, in good agreement with experiment. At intermediate temperatures, 510 K in the model, the two competing mechanisms cancel. The higher dissociation rate of step dimers on the B-step counterbalances the higher density of step adaton1s on this step in such a way that the A- and the B-steps grow at the same speed. The resulting island shape is a hexagon. At high temperatures where all kink dissociations are activated, there will be an equilibrium density of step islands on the two steps, and the island take on its equilibrium shape. Because the model ratio of the step energies agrees with the experimental value, the model reproduces the experimental equilibrium island shape.

The model values of the energy barriers for kink dissociations where chosen to: 1) be in reasonable agreement with the scaled EMT values from [15], 2) agree with the experimental ratio $\varepsilon^{B}_{step}/\varepsilon^{A}_{step}$, and 3) to get agreement with the temperatures at which triangular islands having B-step edges, and the equilibrium island shape, are observed.

While the mechanisms we propose certainly succeed in reproducing the experimental island shapes, they are not necessarily the only set of mechanisms which can do this. At the lower temperatures, there is a limited number of active

processes. Using the kMC simulations, it is possible to test the influence of each process on the island shape, and on this basis, we can draw reliable conclusions concerning what gives rise to the low temperature island shapes. As the temperature is increased, more processes are activated, and this opens up more possibilities for the shape governing mechanisms. We have proposed that the high temperature triangular islands surrounded by B-steps grow because of a high rate of dissociation of step dimers on the B-steps. An alternative mechanism would be that the step dimers are mobile at this temperature. Assuming the same energy levels as in the model presented above, the step dimers could possibly diffuse as entities from the B-steps to the A-steps rather than dissociate and move as step adatoms. Villarba [31] has proposed another model for the rotation of the triangular islands when going from 400 K to 640 K. She also suggests that the step adatoms bind stronger to the B-step at around 400 K. However, the difference in free energy of having an adatom on the two types of steps, could change sign when going to 640 K. This would make step adatoms tend to diffuse to the A-step at the higher temperatures, and could be the origin of the change in island shape.

The growth mode

Having discussed the island shape, we now turn to the growth mode. Figure 5 shows the step density as a function of total deposition for two surface temperatures, 255 K and 370 K. At the lower temperature we observe an oscillating step density, at the higher temperature a monotonically increasing step density. This agrees with the He scattering experiment reported in [18], and shows that the transition to reentrant layer-by-layer growth is reproduced in the model. This is confirmed by Figure 6, which shows the surface morphology at the same two temperatures after the deposition of 0.25 and 4.0 ML. Fig-ure 6 also shows a histogram of the coverages in each layer above the initial surface. It is clear that a more smooth surface is grown at 255 K compared to 370 K in the simulations.

This growth mode transition comes about in the model for the following reason. There are two different inter-layer diffusion processes with different energy barriers in the model. The barrier for an atom to descend from the straight steps is 0.60 eV. This is too high to be overcome even at 370 K. This process is inactive in the simulations, and the exact value of the barrier is insignificant below 400 K, as long as it is not too low. A lower barrier is found for atoms to descend from an island, when the atom is above a kink at a B-step. The model value for this barrier is essentially the scaled EMT barrier from [15], but corrected for the fact that an additional binding of adatoms above descending steps is not included here. This barrier is sufficiently low to be overcome at 255 K. Along the edges of the dendritic islands grown at 255 K this special site is found in abundance, and the total inter-layer diffusion is sufficiently fast to obtain the layer-by-layer growth mode. However, at 370 K where triangular islands having A-step edges are grown, the availability of the low descent-barrier sites is extremely limited. As a result, the inter-layer diffusion is slow, and multilayer growth results. Thus, the transition to reentrant layer-by-layer growth is observed as a direct consequence of the transition in island shape.

The simplest possible model for the inter-layer diffusion is to assume, that atoms have to overcome a constant barrier independent of the local structure of the island edge. By varying this barrier height, the corresponding pre-exponential, and using the model for the in-layer diffusion presented above, it has proven impossible to reproduce the transition to reentrant layer-by-layer growth under this assumption. It is necessary to include some low-barrier process in which the atoms can descend from the dendritic islands.

Figure 7 shows the EMT energy barriers for various descent processes from small compact islands and from straight steps. In EMT it is always easier to descend from the A-step by jumping over the edge. The barrier for this process is around 0.40 eV, rather independent of the size of the island and the presence of kinks or corners. On the B-step however, the lowest descent barrier is always found for the exchange process, in which the descending atom is incorporated in the step, and a step edge atom is pushed out. Figure 7 shows the barriers for such processes at B-steps, when the descending atom is initially directly above a kink site (crosses), above the atom next to the kink site (stars), and further away from any kink site (squares). The kink site can be a corner of an island. Clearly, the EMT descent barriers are insensitive to the island size. Only one descent process has a reduced barrier, and this is the exchange descent at B-steps next to kink sites or island corners. This process also has a low barrier in the Corrected Effective Medium Theory [19], and in the Embedded Atom calculations of Villarba and Jonsson [32]. In the latter potential, a low descent barrier is also found at kinks at A-steps.

Based on the EMT calculations, the present growth model includes a low descent barrier at kinks and corners at the B-steps only. However, we have tried a model which includes the low descent barrier at all kink and corner sites. In such a model, it is possible to reproduce the transition to reentrant layer-by-layer growth only when the descent process at the kink sites has a very low barrier height, and a pre-exponential which is two orders of magnitude lower than for all other processes. The reason for this is the relatively large number of kink sites along the A-step edges of the triangular islands at 370 K. If a low barrier descent process is found at these kink sites, it strongly favors 2D growth at this temperature.

Even when the low barrier descent process is only found at corners and kinks at B steps nucleation of islands in the second layer does not set in for coverages below 0.25 ML at 370 K. Until this point, atoms arriving on top of islands

descend via this low barrier descent process. Since this is almost exclusively found at the tips of the triangular islands, the inter-layer diffusion contributes the growth of these tips.

Summary

In conclusion, we have constructed a model for homo-epitaxial growth of Pt(111) which reproduces experimental island densities, all the observed dendritic and compact island shapes, and the transition in growth mode from 3D growth around 400 K to reentrant layer-by-layer growth at lower temperatures. This model is based on the models in the references [6, 13, 15], each of which deals with only a part of the growth processes. We have obtained a consistent set of diffusion parameters, and we can reproduce the experiments by varying only the deposition flux and substrate temperature. The model has a considerable number of parameters. We have used the EMT result for the edge diffusion processes, that the energy barrier increases with the in-layer coordination of the moving atom. Because of this, it is possible to separate the effects of corner diffusion, step diffusion, and kink dissociations, and draw conclusions concerning the shape governing mechanisms. We want to emphasize our conclusions for these mechanisms, rather than the accuracy of the model values for the diffusion parameters.

Acknowledgments

Stimulating discussions with Hannes Jonsson, George Comsa, and Horia Metiu are gratefully acknowledged. The Center for Atomic-scale Materials Physics is sponsored by The Danish National Research Foundation.

References

[1] Bartelt MC, Evans JW (1994). Dendritic islands in metal on metal epitaxy II. Coalescence and multilayer growth. Surf. Sci. **314**, L835-L842.

[2] Bassett DW, Webber PR (1978). Diffusion of single adatoms of platinum, iridium, and gold on platinum surfaces. Surf. Sci. **70**, 520-531.

[3] Bott M, Hohage M, Michely T, Comsa G (1993). Pt(111) reconstruction induced by enhanced Pt gas phase chemical potential. Phys. Rev. Lett. **70**, 1489-1492.

[4] Bott M, Hohage M, Morgenstern M, Michely T, Comsa G (1996) New approach for determination of diffusion parameters of adatoms. Phys. Rev. Lett. **76**, 1304-1307.

[5] Bott M, Michely T, Comsa G (1991). The homo-epitaxial growth of Pt on Pt(111) studied with STM. Surf. Sci. **272**, 161-166.

[6] Brune H, Röder H, Bromann K, Kern J, Jacobsen J, Stoltze P, Jacobsen K, Nørskov J (1996). Anisotropic corner diffusion as origin for dendritic growth on hexagonal substrates. Surf. Sci. **349**, L115-L122.

[7] Ehrlich G (1995). Atomic events at lattice steps and clusers: A direct view of crystal growth processes. Surf. Sci. 331 333, 865-877.

[8] Esch S, Michely T, Hohage M, Comsa G (1996). The effect of surface reconstruction on the growth mode in homoepitaxy. Surf. Sci. **349**, L89-L94.

[9] Feibelman P (1995). Energetics of steps on Pt(111). Phys. Rev. B **52** 16845-16854.

[10] Feibelman PJ, Nelson JS, Kellogg GL (1994). Energetics of Pt adsorption on Pt(111). Phys. Rev. B **49** 10548-10556.

[11] Fichthorn KA Weinberg WH (1991). Theoretical foundations of dynamical Monte Carlo simulations. J. Chem. Phys. **95**, 1090-1096.

[12] Hohage M, Bott M, Morgenstern M, Zhang Z, Michely T, Comsa G (1996). Atomic processes in low temperature Pt dendrite growth on Pt(111). Phys. Rev. Lett. **76**, 2366-2369.

[13] Jacobsen J, Jacobsen KW, Nørskov JK (1996). Island shapes in homoepitaxial growth of Pt(111). Surf. Sci. **359**, 37-44.

[14] Jacobsen J, Jacobsen KW, Stoltze P (1994). Nucleation of the Pt(111) reconstruction: A simulation study. Surf. Sci. **317**, 8-14.

[15] Jacobsen J, Jacobsen KW, Stoltze P, Nørskov JK (1995). An island shape-induced transition from 2d to 3d growth for Pt/Pt(111). Phys. Rev. Lett. **74**, 2295- 2298.

[16] Jacobsen KW (1988). Bonding in metallic systems: An effective medium approach. Comments Cond. Mat. Phys. **14**, 129-161.

[17] Jacobsen KW, Nørskov, Puslka MJ (1987). Interatomic interactions in the effective-medium theory. Phys. Rev. B **35**, 7423-7442.

[18] Kunkel R, Poelsema B, Verheij LK, Comsa G (1990). Reentrant layer-by-layer growth during molecular-beam epitaxy of metal-on-metal substrates. Phys. Rev. Lett. **65**, 733-736.

[19] Li Y, DePristo AE (1994). Potential energy barriers for interlayer mass transport in homoepitaxial growth on fcc(111) surfaces: pt and Ag. Surf. Sci. **319**, 141-148.

[20] Liu S, Zhang Z, Comsa G, Metiu H (1993). Kinetic mechanism for island shape variations caused by changes in the growth temperature. Phys. Rev. Lett. **71**, 2967-2970.

[21] Liu S, Zhang Z, Nørskov, Metiu H (1994). The mobility of Pt atoms and small Pt clusters on Pt(111) and its implications for the early stages of epitaxial growth. Surf. Sci. **321**, 161-171.

[22] Maksym PA (1988). Fast Monte Carlo simulations of MBE growth. Semicond. Sci. Technol. **3**, 594-596.

[23] Michely T, Comsa G (1991). Temperature dependence of the sputtering morphology of Pt(111). Surf. Sci. **256**, 217-226.

[24] Michely T, Hohage M, Bott M, Comsa G (1993). Inversion of growth speed anisotropy in two dimensions. Phys. Rev. Lett. **70**, 3943-3946.

[25] Mortensen JJ, Hammer B, Stoltze P, Nielsen OH, Jacobsen KW, Nørskov JK (1996) Density Functional Theory Study of Self diffusion on the (111) Surfaces of Ni, Pd, Pt, Cu, Ag and Au, The 18th Taniguchi Symposium on "Elementary Processes in Exitations and Reactions on Solid Surfaces." A. Okiji (ed.). Springer Verlag,

[26] Parmeter JE, Kunkel R, Poelsema B, Verheij LK, Comsa G (1990). Morphology of a Pt(111) Surface during its growth from the vapor phase. Vacuum **41**, 467-470.

[27] Rosenfeld G, Becker A, Poelsema B, Verheij LK, Comsa G (1992). Magic clusters in two-dimensions? Phys. Rev. Lett. **69**, 917-920.

[28] Schwoebel RL (1969). Step motion on crystal surfaces. J. Appl. Phys. **40**, 614-618.

[29] Stoltze P (1994). Simulations of surface defects. J. Phys. Condensed Matter **6**, 9495-9517.

[30] Tersof J, Denier van der Gon AW, Tromp RM (1994). Critical island size for layer-by-layer growth. Phys. Rev. Lett. **72**, 266-269.

[31] Villarba M (1995). PhD thesis, University of Washington, Seattle.

[32] Villarba M, Jonsson H (1994). Diffusion mechanisms relevant to metal crystal growth: Pt/Pt111). Surf. Sci. **317**, 15-36.

[33] Villarba M, Jonsson H (1994) Low-temperature homo-epitaxial growth of pt(111) in simulated vapor deposition. Phys. Rev. B **49**, 2208-2211.

[34] Villarba M, Jonsson H (1995). Atomic exchange processes in sputter deposition of Pt on Pt(111). Surf. Sci. **324**, 35-46.

[35] Voter AF (1986). Classically exact overlayer dynamics: Diffusion of rhodium clusters on Rh(100). Phys. Rev. B **34**, 6819-6829.

[36] Smilauer P, Wilby MR, Vvedensky DD (1993). Reentrant layer-by-layer growth: A numerical study. Phys. Rev. B **47**, 4119-4122.

[37] Wang SC, Ehrlich G (1991). Atom incorporation at surface clusters: An atomic view. Phys. Rev. Lett. **67**, 2509-2512.

[38] Witten TA, Sander LM (1981). Diffusion-limited aggregation, a kinetic critical phenomenon. Phys. Rev. Lett. **47**, 1400-1403.

[39] Zhang Z, Chen X, Lagally MG (1994). Bonding-geometry dependence of fractal growth on metal surfaces. Phys. Rev. Lett. **73**, 1829-1832.

Editor's Note: All reviewers' comments were answered by text changes, hence there is no **Discussion with Reviewers**.